7072 *Biochemistry* **2009,** *48,* 7072–7078
DOI: 10.1021/bi900818a

BIOCHEMISTRY
including biophysical chemistry & molecular biology
Article

Pyroglutamate Formation Influences Solubility and Amyloidogenicity of Amyloid Peptides

Dagmar Schlenzig,[‡] Susanne Manhart,[‡] Yeliz Cinar,[§] Martin Kleinschmidt,[‡] Gerd Hause,[∥] Dieter Willbold,[§,⊥] Susanne Aileen Funke,[§] Stephan Schilling,*[,‡] and Hans-Ulrich Demuth[‡]

[‡]*Probiodrug AG, Weinbergweg 22, 06120 Halle/Saale, Germany,* [§]*Forschungszentrum Jülich, ISB-3, 52428 Jülich, Germany,* [⊥]*Institut für Physikalische Biologie, Heinrich-Heine-Universität, 40225 Düsseldorf, Germany, and* [∥]*Biozentrum der Martin-Luther-Universität, Weinbergweg 22, 06120 Halle/Saale, Germany*

Received May 12, 2009; Revised Manuscript Received June 10, 2009

ABSTRACT: N-Terminally truncated and pyroglutamate (pGlu) modified amyloid β (Aβ) peptides are major constituents of amyloid deposits in sporadic and inherited Alzheimer's disease (AD). Formation of pGlu at the N-terminus confers resistance against cleavage by most aminopeptidases, increases toxicity of the peptides, and may seed Aβ aggregate formation. Similarly, the deposited amyloid peptides ABri and ADan, which cause a very similar histopathology in familial British dementia (FBD) and familial Danish dementia (FDD), are N-terminally blocked by pGlu. Triggered by the coincidence of pGlu-modified amyloid peptides and similar pathology in AD, FBD, and FDD, we investigated the impact of N-terminal pGlu on biochemical and biophysical properties of Aβ, ABri, and ADan. N-Terminal pGlu increases the hydrophobicity and changes the pH-dependent solubility profile, rendering the pGlu-modified peptides less soluble in the basic pH range. The pGlu residue increases the aggregation propensity of all amyloid peptides as evidenced by ThT fluorescence assays and dynamic light scattering. The far-UV CD spectroscopic analysis points toward an enhanced β-sheet structure of the pGlu-Aβ. Importantly, changes in fibril morphology are clearly caused by the N-terminal pGlu, resulting in the formation of short fibers, which are frequently arranged in bundles. The effect of pGlu on the morphology is virtually indistinguishable between ABri, ADan, and Aβ. The data provide evidence for a comparable influence of the pGlu modification on the aggregation process of structurally different amyloid peptides, thus likely contributing to the molecularly distinct neurodegenerative diseases AD, FBD, and FDD. The main driving force for the aggregation is apparently an increase in the hydrophobicity and thus an accelerated seed formation.

The formation of pyroglutamate (pGlu)[1] is a common post-translational modification of several peptide hormones and proteins. The residue influences the structure and physiological function by mediating an interaction with receptors and/or stabilizes peptides against N-terminal degradation (*1*). The accumulation of pGlu-amyloid peptides in neurodegenerative disorders like Alzheimer's disease (AD), familial British dementia (FBD), and familial Danish dementia (FDD) has been implicated to contribute to the formation of amorphous and fibrillar deposits, which represent a characteristic hallmark of these disorders (*2*−*4*).

The amyloid β peptide (Aβ) is the major component of plaques in AD. The peptide is produced by sequential endoproteolytic processing of the precursor protein APP by β- and γ-secretase. An alternative cleavage by γ-secretase at various sites results primarily in Aβ40 and Aβ42, species that differ at their C-termini. Among these, Aβ42 shows the highest aggregation propensity, and its deposition precedes that of Aβ40 *in vivo* (*5*). In addition, N-terminal heterogeneity is caused by alternative cleavage of APP by the β-secretase BACE at the so-called β- and β'-position, generating Aβ1−40/42 or Aβ11−40/42, respectively. Previous reports point toward formation of other N-truncated Aβ peptides from APP, e.g., Aβ5−40/42 and Aβ3−40/42 by yet undiscovered mechanisms (*6*, *7*). The truncated Aβ peptides show an enhanced aggregation propensity compared to full-length peptides (*8*−*12*). Among these, pGlu-modified peptides are prominent in AD and have been postulated to initiate amyloid plaque formation (*3*, *13*). Very recent results underline this important role of pGlu-Aβ for the plaque formation and progression of Alzheimer's-like pathology in mice (*14*).

Interestingly, also the deposits in the inherited neurodegenerative disorders FBD and FDD consist mainly of pGlu-modified amyloid. The generation of the peptides ABri and ADan is due to processing of a mutated *BRI*$_2$ gene. Both peptides are not related to Aβ in terms of their primary structure (*15*, *16*). ABri and ADan share an identical N-terminal sequence of 22 amino acids but have different C-termini of 12 amino acids. Following processing of the BRI2 protein by furin-like protease(s), an N-terminal glutamic acid residue is generated. Reminiscent of

*To whom correspondence should be addressed. Phone: 49 345 5559911. Fax: 49 345 5559901. E-mail: stephan.schilling@probiodrug.de.

[1]Abbreviations: Aβ, amyloid β; AD, Alzheimer's disease; FBD, familial British dementia; FDD, familial Danish dementia; pGlu, pyroglutamate.

 Published on Web 06/11/2009

Table 1: Sequences of Amyloid Peptides Aβ, ADan, and ABri, Their Theoretical Isoelectric Points, and Retention Times in Reversed-Phase HPLC[a]

peptide	sequence	theoretical p*I*	RT (min) (method)
Aβ1−40	DAEFRHDSGYEVHHQKLVFFAEDVGSNKGAIIGLMVGGVV	5.31	16.4 (a)
Aβ3−40	EFRHDSGYEVHHQKLVFFAEDVGSNKGAIIGLMVGGVV	5.78	16.1 (a)
pGlu-Aβ3−40	pEFRHDSGYEVHHQKLVFFAEDVGSNKGAIIGLMVGGVV	6.30	19.7 (a)
Aβ11−40	EVHHQKLVFFAEDVGSNKGAIIGLMVGGVV	6.02	16.9 (a)
pGlu-Aβ11−40	pEVHHQKLVFFAEDVGSNKGAIIGLMVGGVV	7.32	17.6 (a)
Glu[1]-ADan	EASNCFAIRHFENKFAVETLICFNLFLNSQEKHY	6.05	13.7 (b)
pGlu[1]-ADan	pEASNCFAIRHFENKFAVETLICFNLFLNSQEKHY	7.24	14.5 (b)
Glu[1]-ABri	EASNCFAIRHFENKFAVETLICSRTVKKNIIEEN	6.85	10.6 (b)
pGlu[1]-ABri	pEASNCFAIRHFENKFAVETLICSRTVKKNIIEEN	8.40	12.1 (b)

[a] For methods a and b see Experimental Procedures.

Aβ in Alzheimer's disease, the N-terminus of ABri and ADan is then converted into pGlu, representing the dominant species in the amyloid deposits in FBD and FDD (*4*).

In general, the pGlu modification is prominent at the N-terminus of secreted amyloid peptides in different neurodegenerative disorders. The aim of the present study was to analyze the influence of the modified N-terminus on the characteristics of the dementia-related amyloid peptides pGlu-Aβ3−40, pGlu-Aβ11−40, pGlu-ABri, and pGlu-ADan. With respect to Aβ, we focused on *x*−40 species because of their better solubility and lower aggregation propensity compared to Aβ*x*−42, which enabled a reliable investigation of the influence of the peptide N-terminus in aqueous buffer solution. The biophysical properties of the peptides were compared in order to gain further information regarding the role of the modification for development of neurodegenerative diseases. The peptide sequences are summarized in Table 1.

EXPERIMENTAL PROCEDURES

Materials. Aβ peptides were synthesized as described previously (*11*). pGlu-ABri was purchased from Bachem (Bubendorf, Switzerland). All chemicals used were of analytical grade.

Synthesis of ADan, pGlu-ADan, and ABri. The peptides were synthesized in 50 μmol scale on a Fmoc-Tyr-NovaSyn-TGA resin using an automated Symphony synthesizer (Rainin). After deprotection and purification by HPLC, the disulfide bond was introduced by iodine oxidation. The peptides were dissolved in AcOH/H_2O (4:1) to a final concentration of about 2 mg/mL. Ten equivalents of iodine was added at once, and the mixture was stirred for up to 1 h at room temperature. Completion of oxidation was followed by HPLC and MALDI-TOF mass spectrometry. The reaction was quenched by diluting the reaction volume twice with H_2O, and the iodine was extracted with tetrachlormethane (at least five to six times). The resulting aqueous phase was lyophilized and purified by preparative HPLC using a gradient of acetonitrile in H_2O containing 0.04% TFA. Analytical HPLC for determining retention time (Table 1) was carried out with two different methods. Method a: 4.6 × 150 Source 5RPC column (5 μm; GE Healthcare) with a gradient made of solvent B (60% acetontrile/40% solvent A) and solvent A (0.1% NH_4OH in H_2O at pH 9); 10% B for 1 min and 10−100% B in 30 min (detection 220 nm, flow 1 mL/min, column temperature 35 °C). Method b: 125 × 4 Luna C18(2) column (5 μm; Phenomenex) with a gradient made of solvent A (acetonitrile containing 0.04% TFA) and solvent B (H_2O containing 0.04% TFA); 5−50% A in 15 min, 50−70% A in 17 min (detection 214 nm, flow 1 mL/min, column temperature 25 °C).

Solubility Test. The assessment of peptide solubility was performed, essentially as described by Hortschansky et al. (*17*). Briefly, MES/Tris/acetate buffer (50 mM, 100 mM, 50 mM) was prepared (pH 3.5, 4.0, 4.5, 5.0, 5.5, 6.0, 6.5, 7.0, 7.5, 8.0, 8.5, 9.0). This buffer provides a constant ionic strength in the pH range of investigation (*18*). The amyloid peptides were dissolved in water (150 μM) and mixed with buffer 2:1 to a final concentration of 75 μM (total volume 100 μL). The solutions were divided, and one part was centrifuged for 30 min at 14000 rpm. Samples of 30 μL of supernatant were removed for peptide quantification by Micro-BCA assay (Pierce). For the Micro-BCA assay, samples of 10 μL were incubated with 150 μL of working solution and analyzed according to the guidelines of the manufacturer. The analysis was performed in duplicate, and peptide concentrations were calculated using a standard curve of BSA under assay conditions. Results were expressed as percent of total peptide concentration.

Preparation of Seedless Amyloid Peptide Stock Solutions. The amyloid peptides were dissolved in HFIP (1 mM) and incubated for 2 h at room temperature. The concentration was determined by absorption at 280 nm, applying an extinction coefficient of 1490 M^{-1} cm^{-1} for Aβ*x*−40 and 1615 M^{-1} cm^{-1} for ADan, making use of the absorption by the side chains of aromatic amino acids. ABri solutions were prepared on the basis of peptide mass, because a suitable chromophore is lacking. Stock solutions were aliquoted and stored at −80 °C until use. Prior to use, HFIP was evaporated, and peptides were dissolved in 0.1 M NaOH (Aβ*x*−40) or 0.1 M HCl (ADan and ABri). After 10 min of incubation, the analysis buffer was added, and the pH value was adjusted by the addition of 0.1 M HCl or 0.1 M NaOH, respectively (volume of HCl/NaOH solution was 10% of total volume). This method was shown to result in peptide preparations free of aggregates as evidenced by size exclusion chromatography (data not shown). To exclude potential occurrence of oxidative peptide modifications due to the applied pH conditions, MALDI-TOF mass spectrometric analysis of the solutions was applied over a time period of several hours.

Thioflavin T (ThT) Assay. Peptide solutions of 100 μM in MES/Tris/acetate buffer (50 mM, 100 mM, 50 mM, pH 4.0, 7.0, or 8.0) were mixed 2:1 with 40 μM thioflavin T in water, containing 0.01% NaN_3. Final concentration of peptides for measuring aggregation kinetics was 50 μM, and 200 μL was applied per well of a 96-well blackwall microplate. The plate was covered with an adhesive film and incubated in a plate reader at 37 °C. Fluorescence readings were recorded every 2 h for up to 2 weeks (excitation 440 nm, emission 490 nm). Routinely, assays of each peptide were performed in six cavities of one plate, and the mean of the determined fluorescence units was calculated.

Analysis of Secondary Structure by CD Spectroscopy. Circular dichroism spectra were recorded using a Jasco J-710

spectropolarimeter. After seedless preparation, peptide solutions (50 μM) were prepared in 10 mM sodium phosphate buffer at pH 8.0 and incubated at 37 °C. The peptides were applied to a quartz cell of 0.5 mm path length, and the spectra were recorded in the far-UV range (190−260 nm), applying a scan rate of 50 nm/min. For a typical spectrum, 10 scans were accumulated and baseline corrected.

Dynamic Laser Light Scattering (DLS). Seedless amyloid peptide solutions of 5 μM were prepared in 50 mM sodium phosphate buffer containing 100 mM NaCl, pH 7.5. All buffers were filtered (0.22 μm pore size) prior to use. DLS measurements were carried out with a *DynaPro* dynamic light scattering system (Protein Solutions, Lakewood, NJ) using a 45 μL quartz cuvette with 3 mm path length. Readings were recorded at 20 °C with a fixed angle of 90°. Data acquisition time was 3 s over a period of 10 min using a 655.6 nm (13 mW) laser. Analysis and averaging of the collected data were performed with the software Dynamic V6 (Protein Solutions, Lakewood, NJ). By using calculated autocorrelation functions, a regularization fit was performed in order to obtain the size distribution profile.

Transmission Electron Microscopy. Samples were taken from the aggregation reactions, and the peptide aggregates were adsorbed on Formvar-coated copper grids (Plano GmbH, Wetzlar), washed with distilled water three times, and negatively stained with 1% uranyl acetate. The peptide aggregates were observed using an EM 900 (Carl Zeiss SMT, Oberkochen) operating at 80 kV. Images were taken, applying a Variospeed SSCCD camera SM-1k-120 (TRS, Moorenweis).

RESULTS

pH-Dependent Solubility of Amyloid Peptides. The cyclization of N-terminal glutamic acid into pyroglutamic acid is accompanied by the loss of two functional hydrophilic groups, which potentially influences charge conditions and solvation of the peptides. Caused by the formation of the N-terminal lactam ring, the basicity of the N-terminal amino group and the negative charge of the carboxyl group get lost. Consequently, the cyclization exerts an effect on the calculated isoelectric points (p*I*) of the amyloid peptides ADan, ABri, and Aβ, rendering the pI of the peptides more basic as illustrated in Table 1. The modification of the N-terminus also increases the retention time during reversed-phase HPLC, suggesting an increase of hydrophobicity of the pyroglutamated peptides. The N-terminal cyclization of glutamic acid thus influences all amyloid peptides under investigation in a similar manner by increasing their hydrophobicity. The change of the retention time and, in turn, the increase of the hydrophobicity were most prominent for pGlu-Aβ3−40 and pGlu-ABri. Generally, the solubility of peptides is lowest in the range of their isoelectric points. This has been demonstrated for Aβ1−40 by Hortschansky et al. (*17*). Caused by the changing p*I*, differences in the pH-dependent solubility profile were observed (Figure 1). Comparing the solubility of Aβ1−40, Aβ3−40, and pGlu-Aβ3−40, a shift of the pH-dependent minima of solubility was found. However, about 60% of the peptide remained in solution in the entire pH range investigated. The truncation of the first 10 amino acids of Aβ1−40 results in a strong reduction in the solubility of both Aβ11−40 and pGlu-Aβ11−40. The differences in their pH-dependent solubility profile are not that pronounced as for the other peptides but statistically significant at pH 7.5 and higher pH values. The pGlu modification renders the Aβ11−40 peptide, however, virtually insoluble in the entire pH range. Accordingly, also the solubility of ADan, pGlu-ADan, ABri, and pGlu-ABri is very poor at pH values close to their isoelectric points.

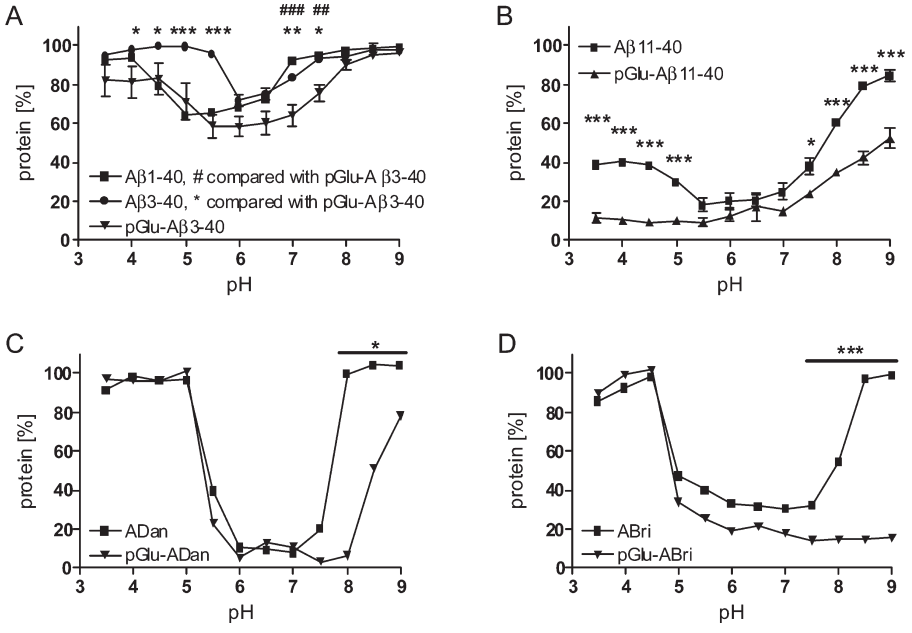

FIGURE 1: Relative solubility of amyloid peptides at room temperature depending on the pH of the aqueous buffered solution. The peptides (75 μM) were dissolved in MES/Tris/acetate buffer (25 mM, 50 mM, 25 mM), the solutions were centrifuged, and the peptide concentration in the supernatant was determined by applying a BCA assay. (A) Solubility of Aβ1−40, Aβ3−40, and pGlu-Aβ3−40 (n = 4). (B) Aβ11−40 compared with pGlu-Aβ11−40 (n = 4). (C) ADan compared with pGlu-ADan (n = 2). (D) ABri compared with pGlu-ABri (n = 2). For all investigated amyloid peptides a decreased solubility of the pGlu-modified peptides in the basic range was found. A statistical analysis was carried out for Aβx−40 and Aβ11−40 by applying a two-way ANOVA followed by a Bonferroni posttest (A, B). The method allowed a comparison of the solubility at every pH value based on the four determinations in parallel. A statistical evaluation of the solubility of ABri and ADan was achieved by applying an unpaired Student's t test (C, D). The statistical significant difference thus refers to a pH range and not to a distinct pH value. Key: ### and *** for $P < 0.001$, ## and ** for $P < 0.01$, and * for $P < 0.05$.

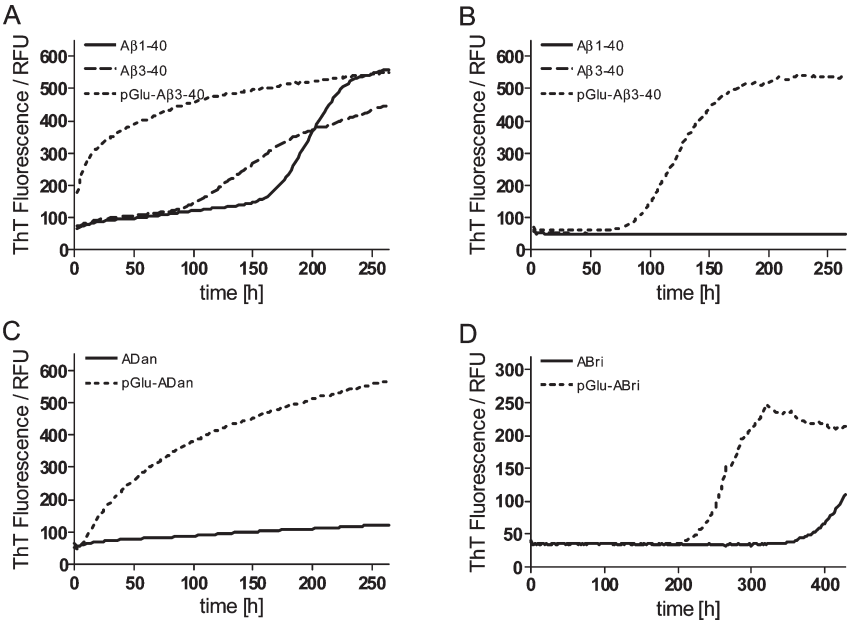

FIGURE 2: Aggregation kinetics of Aβ, ADan, and ABri monitored by ThT fluorescence. The peptides (50 μM) were dissolved in MES/Tris/acetate buffer (25 mM, 50 mM, 25 mM) containing 20 μM ThT at 37 °C. (A) Aggregation of Aβ1−40, Aβ3−40, and pGlu-Aβ3−40 at pH 7.0. A lag phase was not observed for pGlu-Aβ3−40. (B) Aggregation of Aβ1−40, Aβ3−40, and pGlu-Aβ3−40 at pH 8.0. In contrast to Aβ1−40 and Aβ3−40, pGlu-Aβ3−40 formed fibrillar aggregates after a lag phase of 70 h. (C, D) Aggregation of ADan, pGlu-ADan and ABri, pGlu-ABri at pH 4.0. The peptides with an unmodified N-terminus aggregated much slower than the pE peptides.

Aggregation Propensity of Amyloid Peptides. The changes in the solubility profile reflect the influence of N-terminal pGlu on hydrophobicity and solvation of the amyloid peptides, which might affect the nucleation process. Accordingly, we were questioning whether this has an impact on the aggregation kinetics. The fibril formation from monomeric Aβ1−40, Aβ3−40, and pGlu-Aβ3−40 (50 μM) was investigated by a ThT fluorescence assay at pH 7.0 and 8.0, because the differences of the pH-dependent solubility profile were largest at these values (Figure 1). Aβ11−40 and pGlu-Aβ11−40 could not be reliably analyzed because of the poor overall solubility in the physiological pH range.

At pH 7.0, fibrils are very rapidly generated from pGlu-Aβ3−40, as suggested by the increase of the fluorescence intensity (Figure 2). The typical lag phase, i.e., the phase in which oligomers and protofibrils are slowly formed and act as seeds for the growing fibrils, could not be detected, indicating an instant seeding of the aggregation process. Aβ1−40, which shows better solubility at pH 7.0, aggregates with a prominent lag phase. Similarly, such fibril formation has been also observed with Aβ3−40. The truncation results in a shortened lag phase but slower fibril elongation as concluded by the lower slope in the exponential phase. Thus, the truncation seems to accelerate the seed formation process, which is further enhanced by the cyclization of N-terminal glutamic acid. The changes are also in good agreement with the differences in solubility profiles (Figure 1). At pH 8.0, pGlu-Aβ3−40 shows characteristic fibrillation kinetics with a lag phase of 70 h. The lag phase of fibril formation from Aβ1−40 and Aβ3−40 is increased to a value out of the measurement range. A formation of fibrils has been verified for all samples using electron microscopic analysis after incubation at 37 °C for 14 days (data not shown). Despite the apparently similar solubility at pH 8.0, there are dramatic differences in the aggregation kinetics of the investigated Aβ peptides. However, it should be considered that the characterization of the solubility of the peptides did not aim at determination of a limiting concentration. Hence, the peptides might still differ with regard to the total solubility at very basic and acidic pH.

Comparing the aggregation kinetics of ADan with pGlu-ADan and ABri with pGlu-ABri at pH 4.0, i.e., at a pH where the peptides are well soluble, a dramatic influence of N-terminal pGlu in the case of ADan was observed. pGlu-ADan aggregated without a lag phase, whereas ADan did not form fibrils during the time period of investigation. pGlu-ABri formed fibrils much slower than pGlu-ADan. Moreover, the initial lag phase was doubled if the N-terminal glutamic acid was not converted into pGlu in ABri.

In order to corroborate the findings of the ThT fluorescence assays, an analysis of the aggregation process was performed, applying dynamic light scattering (DLS) for investigation of Aβ1−40, Aβ3−40, and pGlu-Aβ3−40 and for comparative purposes with Aβ1−42. As shown in Figure 3, in accordance with the greater aggregation propensity of pGlu-Aβ3−40 measured in the ThT assay, DLS measurements at a 5 μM peptide concentration revealed a fast occurrence of larger aggregates in the pGlu-Aβ sample at time point 0. After 24 h, pGlu-Aβ already shows additional aggregates in the size range of 10^3−10^4 nm. Aggregates with similar hydrodynamic radii appear with Aβ1−42 and Aβ3−40 in a time frame of 48 h and later with Aβ1−40.

Investigation of Conformational Changes of Aβ. In a previous study, CD spectroscopic analysis was used to characterize the structural changes of Aβ during the aggregation process (*19*). In order to investigate the influence of N-terminal pGlu on the structural rearrangements of Aβ, a CD spectroscopic analysis of Aβ1−40 and pGlu-Aβ3−40 was performed. The rapid aggregation of pGlu-Aβ3−40 compared to Aβ1−40 is accompanied by faster structural changes as seen in these experiments. Both peptides are initially in random coil structure. Conformational changes of the pGlu-Aβ-containing sample started after day 3. The first structural changes of Aβ1−40 were observed on day 5, and the transition was finished after 12 days.

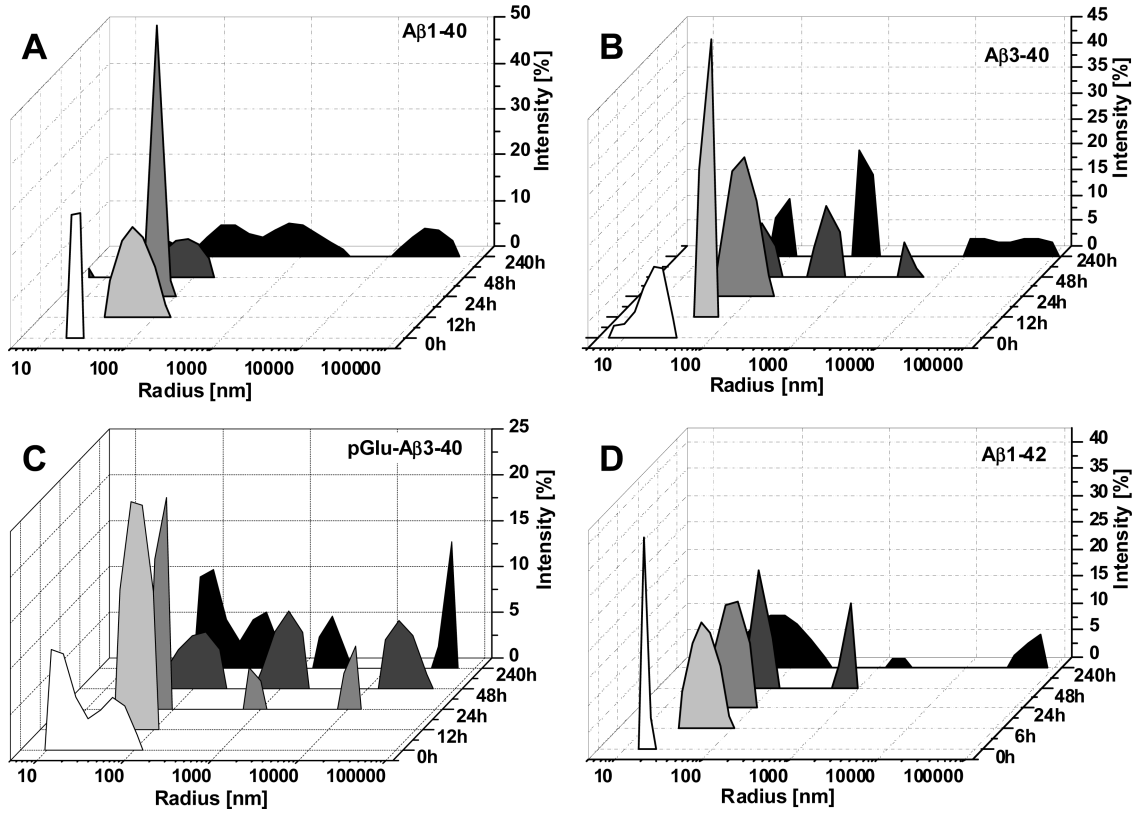

FIGURE 3: Aggregation of different Aβ species monitored by dynamic light scattering (DLS). The peptides (5 μM) were dissolved in 50 mM phosphate buffer, pH 7.5, containing 100 mM NaCl and incubated at 37 °C. Formation of large aggregates with hydrodynamic radii of 10^3−10^5 nm was fastest for pGlu-Aβ3−40 followed by Aβ3−40, Aβ1−42, and Aβ1−40.

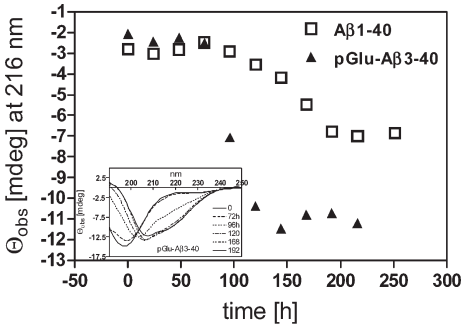

FIGURE 4: Structural changes accompanying the aggregation process of Aβ as assessed by CD spectroscopy. Aβ1−40 and pGlu-Aβ3−40 (50 μM) were incubated at 37 °C in 10 mM phosphate buffer, and the ellipticity was measured at 217 nm. The β-sheet content of pGlu-Aβ3−40 increases rapidly and in a similar time frame, in which aggregate formation was observed in the ThT assay. Structural changes of Aβ1−40 were slower. Inset: Time course of CD spectra of pGlu-Aβ3−40 during aggregation.

The lower negative CD signal at 217 nm clearly supports a significantly higher β-sheet content in pGlu-Aβ3−40 compared with Aβ1−40 (Figure 4). The lack of a dichroic point in the pGlu-Aβ3−40 sample is indicative for more than two conformations involved in conformational conversion, pointing to a different aggregation mechanism or intermediate pathways of pGlu-Aβ3−40 as compared with Aβ1−40.

Comparative Evaluation of the Fibril Morphology. To evaluate the effect of N-terminal pGlu on the morphology of the fibrils formed by amyloid peptides, negatively stained samples were analyzed by transmission electron microscopy. Amyloid peptides without N-terminal pGlu show the typical morphology

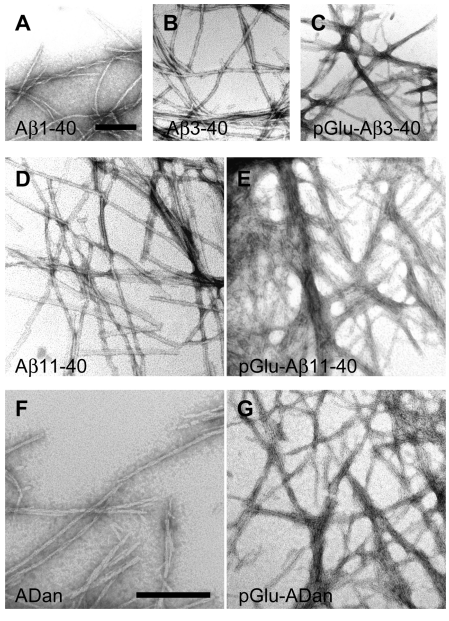

FIGURE 5: Electron micrographs of negatively stained amyloid aggregates generated with Aβ1−40, Aβ3−40, pGlu-Aβ3−40, Aβ11−40, pGlu-Aβ11−40, ADan, and pGlu-ADan. Fibrils were generated in MES/Tris/acetate buffer (25 mM, 50 mM, 25 mM, pH 7.0 or 4.0). Scale bars indicate 200 nm; the magnification was 85000×.

of mature fibrils (Figure 5 A,B,D,F). The fibrils are smooth and partially twisted. Interestingly, also Aβ11−40 fibrils (Figure 5 D) did not show a different morphology, although the truncation of the Aβ peptide N-terminal part led to a dramatic decrease of solubility (compare Figure 1). In contrast, however, the pGlu

modification resulted in a significant change of fibril morphology (Figure 5 C,E,F).

The aggregates form a dense meshwork of short fibrils that self-associate laterally to form irregular bundles. The fibrils formed from ADan are similar to Aβ in general appearance. Interestingly, although the peptide does not have similarity to Aβ regarding its primary structure, the pGlu residue affects the fibril morphology in a comparable manner. The pGlu modification leads to formation of very short fibrils and lateral association of the fibrils (Figure 5). Thus, it appears that the pGlu modification does not only increase the tendency of aggregation in general but apparently affects the surface properties of fibrils promoting interfibril interactions.

DISCUSSION

The C-terminal heterogeneity of Aβ peptides and its role in the pathogenesis of the Alzheimer's dementia are well characterized and represent a basis for delineation of treatment strategies of AD aiming at, for instance, reduction of Aβ42 (*20*−*22*). The role of the prominent N-terminal heterogeneity of Aβ, however, is not that well understood. Different studies suggest that N-terminal truncation and modification influence the aggregation propensity, seeding capacity, and toxicity of these peptides (*8*, *9*, *11*, *23*). In particular, pGlu-Aβ might have disease-provoking potential due to its abundance and correlation with severity of AD (*2*, *5*, *12*, *13*, *24*). Interestingly, pGlu-modified amyloid is also dominant in FBD and FDD. About 90% of ABri and ADan in systemic and brain deposits is N-terminally blocked. Similar to AD, the N-terminus is generated by cyclization of an N-terminal glutamic acid residue. However, the soluble peptide, which is present in high concentrations in the circulation, carries an unmodified N-terminus (*4*, *25*). These observations support the hypothesis that amyloid peptides with N-terminal pGlu play a crucial role in the pathogenesis of the amyloid-derived dementias FBD, FDD, and AD. A more detailed knowledge on the influence of the N-terminal modification on the biophysical properties of the nonrelated amyloid peptides Aβ, ADan, and ABri was the aim of the present study.

A comparative investigation of the different peptide species revealed a decrease of solubility in the physiological pH range caused by the N-terminal pGlu modification, which is accompanied by an increase in hydrophobicity. The differences in solubility are most likely caused by the loss of two charged, hydrophilic groups upon cyclization of glutamic acid. Presumably, the loss of the charges is one of the driving forces of the rapid aggregation of the pGlu-modified amyloid peptides. This is finally evidenced by the comparison of the aggregation propensity of the different amyloid peptides Aβ, ADan, and ABri. Despite their different primary structure the influence of the pGlu N-terminus is very similar. The results thus also implicate that initial hydrophobic intermolecular interactions of these peptides represent one trigger of peptide assembly. This, in turn, might be critical for the situation *in vivo* and supports the potential seeding function of pGlu-Aβ, pGlu-ADan, and pGlu-ABri. Even at pH of elevated solubility, the intrinsic aggregation propensity is higher for the pGlu peptides. On the other hand, cyclization of N-terminal glutamate could account for structural changes of the N-terminal part of the peptides, which increase the nucleation propensity. Previous studies on the supramolecular structure of Aβ aggregates based on proteolytic accessibility and using solvent H/D exchange, carried out by mass spectrometry and NMR techniques, provided evidence for a structurally disordered and solvent-accessible peptide N-terminus in full-length Aβ (*26*−*28*). Introduction of the pGlu, accompanied by reduction of solvent interactions, could constrain this disordered state by stiffening the N-terminus. Although direct evidence for that hypothesis is still lacking, there are data available from other proteins, in which the N-terminal pGlu formation triggers structural rearrangements. In onconase, a frog RNase protein, catalytic activity and cytotoxicity are determined by structural integrity, and this strongly depends on N-terminal pGlu, which tethers the N-terminus into the protein body, i.e., hiding it from the direct accessibility by the solvent, upon folding of the enzyme (*29*, *30*). With regard to Aβ, the differences of the CD spectra of pGlu-Aβ3−40 and Aβ1−40, aggregated under same conditions, point to the formation of different structures. That increased hydrophobicity in the N-terminal part of Aβ has an accelerating impact on the aggregation propensity of Aβ1−40/42 has been shown very recently for an APP mutation that results in an Ala → Val exchange at position 2 of Aβ (*31*). The increase in the hydrophobicity of the N-terminus might also be reflected by the dramatically different fibril morphology of the here investigated amyloid peptides. Interestingly, the change in morphology is not unique to one of these peptides, but it is rather independent from their primary structure, promoting similar interaction modes within the aggregates. The more sticky appearance of pGlu peptides might be caused by interactions of their hydrophobic N-termini. This, in turn, could finally affect not only interfibril interactions but also hydrophobic interactions with cellular proteins, membranes, or other surfaces directly influencing the cytotoxic properties of the peptides.

Protein functionality and resistance to aggregation *in vivo* are thought to represent a fragile homeostasis, which is highly dependent on protein concentration and protein solubility. Aggregation rates are increased either by raised protein concentrations as a result of genetic mutations or impaired regulatory processes or by decreased solubility caused by chemical modifications (*32*). This situation is well reflected in Alzheimer's disease, where mutations that alter physiological Aβ concentrations (i.e., Swedish and London mutation) or increase the concentration of modified Aβ (*31*) result in brain deposits of Aβ and early onset AD. Age-related impaired regulatory processes obviously have the same effects in late-onset AD. According to that hypothesis, pGlu-amyloid peptides, mediated by their diminished solubility, increased hydrophobicity, and probably increased stability, might represent a trigger for the change of homeostasis and initiation of pathophysiology.

Taken together, we have shown for the first time that the pGlu N-terminus of non-Aβ-related amyloid peptides, which also cause neurodegenerative disorders, influences the biophysical properties in a very similar manner as pGlu in Aβ by changing their solubility profile and increasing their hydrophobicity. These characteristics directly affect the aggregation kinetics, changes in secondary structure, and the fibril morphology. The suppression of the pGlu-amyloid formation, e.g., by inhibition of glutaminyl cyclase, might represent, therefore (*33*), a therapeutic strategy to diminish the progression of neurodegenerative amyloidoses like AD, FBD, and FDD.

ACKNOWLEDGMENT

The authors are grateful to Renu Batra-Safferling for support in conducting the DLS experiments.

REFERENCES

1. Schilling, S., Wasternack, C., and Demuth, H. U. (2008) Glutaminyl cyclases from animals and plants: a case of functionally convergent protein evolution. *Biol. Chem. 389*, 983–991.
2. Saido, T. C., Yamao, H., Iwatsubo, T., and Kawashima, S. (1996) Amino- and carboxyl-terminal heterogeneity of beta-amyloid peptides deposited in human brain. *Neurosci. Lett. 215*, 173–176.
3. Saido, T. C., Iwatsubo, T., Mann, D. M., Shimada, H., Ihara, Y., and Kawashima, S. (1995) Dominant and differential deposition of distinct beta-amyloid peptide species, A beta N3(pE), in senile plaques. *Neuron 14*, 457–466.
4. Ghiso, J., Revesz, T., Holton, J., Rostagno, A., Lashley, T., and Houlden, H.; et al. (2001) Chromosome 13 dementia syndromes as models of neurodegeneration. *Amyloid 8*, 277–284.
5. Iwatsubo, T., Saido, T. C., Mann, D. M., Lee, V. M., and Trojanowski, J. Q. (1996) Full-length amyloid-beta (1−42(43)) and amino-terminally modified and truncated amyloid-beta 42(43) deposit in diffuse plaques. *Am. J. Pathol. 149*, 1823–1830.
6. Cescato, R., Dumermuth, E., Spiess, M., and Paganetti, P. A. (2000) Increased generation of alternatively cleaved beta-amyloid peptides in cells expressing mutants of the amyloid precursor protein defective in endocytosis. *J. Neurochem. 74*, 1131–1139.
7. Takeda, K., Araki, W., Akiyama, H., and Tabira, T. (2004) Amino-truncated amyloid beta-peptide (Abeta5−40/42) produced from caspase-cleaved amyloid precursor protein is deposited in Alzheimer's disease brain. *FASEB J. 18*, 1755–1757.
8. Pike, C. J., Overman, M. J., and Cotman, C. W. (1995) Amino-terminal deletions enhance aggregation of beta-amyloid peptides in vitro. *J. Biol. Chem. 270*, 23895–23898.
9. He, W., and Barrow, C. J. (1999) The A beta 3-pyroglutamyl and 11-pyroglutamyl peptides found in senile plaque have greater beta-sheet forming and aggregation propensities in vitro than full-length A beta. *Biochemistry 38*, 10871–10877.
10. Piccini, A., Russo, C., Gliozzi, A., Relini, A., Vitali, A., and Borghi, R.; et al. (2005) {beta}-Amyloid is different in normal aging and in Alzheimer disease. *J. Biol. Chem. 280*, 34186–34192.
11. Schilling, S., Lauber, T., Schaupp, M., Manhart, S., Scheel, E., and Bohm, G.; et al. (2006) On the seeding and oligomerization of pGlu-amyloid peptides (in vitro). *Biochemistry 45*, 12393–12399.
12. Miravalle, L., Calero, M., Takao, M., Roher, A. E., Ghetti, B., and Vidal, R. (2005) Amino-terminally truncated Abeta peptide species are the main component of cotton wool plaques. *Biochemistry 44*, 10810–10821.
13. Russo, C., Schettini, G., Saido, T. C., Hulette, C., Lippa, C., and Lannfelt, L.; et al. (2000) Presenilin-1 mutations in Alzheimer's disease. *Nature 405*, 531–532.
14. Schilling, S., Zeitschel, U., Hoffmann, T., Heiser, U., Francke, M., and Kehlen, A.; et al. (2008) Glutaminyl cyclase inhibition attenuates pyroglutamate Abeta and Alzheimer's disease-like pathology. *Nat. Med. 14*, 1106–1111.
15. Vidal, R., Frangione, B., Rostagno, A., Mead, S., Revesz, T., and Plant, G.; et al. (1999) A stop-codon mutation in the BRI gene associated with familial British dementia. *Nature 399*, 776–781.
16. Vidal, R., Revesz, T., Rostagno, A., Kim, E., Holton, J. L., and Bek, T.; et al. (2000) A decamer duplication in the 3′ region of the BRI gene originates an amyloid peptide that is associated with dementia in a Danish kindred. *Proc. Natl. Acad. Sci. U.S.A. 97*, 4920–4925.
17. Hortschansky, P., Schroeckh, V., Christopeit, T., Zandomeneghi, G., and Fandrich, M. (2005) The aggregation kinetics of Alzheimer's beta-amyloid peptide is controlled by stochastic nucleation. *Protein Sci. 14*, 1753–1759.
18. Ellis, K. J., and Morrison, J. F. (1982) Buffers of constant ionic strength for studying pH-dependent processes, in Methods in Enzymology (Purich, D., Ed.) Vol. 87, pp 405−426, Academic Press, New York.
19. Kirkitadze, M. D., Condron, M. M., and Teplow, D. B. (2001) Identification and characterization of key kinetic intermediates in amyloid beta-protein fibrillogenesis. *J. Mol. Biol. 312*, 1103–1119.
20. Iwatsubo, T., Odaka, A., Suzuki, N., Mizusawa, H., Nukina, N., and Ihara, Y. (1994) Visualization of A beta 42(43) and A beta 40 in senile plaques with end-specific A beta monoclonals: evidence that an initially deposited species is A beta 42(43). *Neuron 13*, 45–53.
21. Selkoe, D. J. (2001) Alzheimer's disease: genes, proteins, and therapy. *Physiol. Rev. 81*, 741–766.
22. McGowan, E., Pickford, F., Kim, J., Onstead, L., Eriksen, J., and Yu, C.; et al. (2005) Abeta42 is essential for parenchymal and vascular amyloid deposition in mice. *Neuron 47*, 191–199.
23. Russo, C., Violani, E., Salis, S., Venezia, V., Dolcini, V., and Damonte, G.; et al. (2002) Pyroglutamate-modified amyloid beta-peptides—AbetaN3(pE)—strongly affect cultured neuron and astrocyte survival. *J. Neurochem. 82*, 1480–1489.
24. Guntert, A., Dobeli, H., and Bohrmann, B. (2006) High sensitivity analysis of amyloid-beta peptide composition in amyloid deposits from human and PS2APP mouse brain. *Neuroscience 143*, 461–475.
25. Ghiso, J. A., Holton, J., Miravalle, L., Calero, M., Lashley, T., and Vidal, R.; et al. (2001) Systemic amyloid deposits in familial British dementia. *J. Biol. Chem. 276*, 43909–43914.
26. Balbach, J. J., Petkova, A. T., Oyler, N. A., Antzutkin, O. N., Gordon, D. J., and Meredith, S. C.; et al. (2002) Supramolecular structure in full-length Alzheimer's beta-amyloid fibrils: evidence for a parallel beta-sheet organization from solid-state nuclear magnetic resonance. *Biophys. J. 83*, 1205–1216.
27. Kheterpal, I., Williams, A., Murphy, C., Bledsoe, B., and Wetzel, R. (2001) Structural features of the Abeta amyloid fibril elucidated by limited proteolysis. *Biochemistry 40*, 11757–11767.
28. Petkova, A. T., Ishii, Y., Balbach, J. J., Antzutkin, O. N., Leapman, R. D., and Delaglio, F.; et al. (2002) A structural model for Alzheimer's beta -amyloid fibrils based on experimental constraints from solid state NMR. *Proc. Natl. Acad. Sci. U.S.A. 99*, 16742–16747.
29. Arnold, U., Schulenburg, C., Schmidt, D., and Ulbrich-Hofmann, R. (2006) Contribution of structural peculiarities of onconase to its high stability and folding kinetics. *Biochemistry 45*, 3580–3587.
30. Liao, Y. D., Wang, S. C., Leu, Y. J., Wang, C. F., Chang, S. T., and Hong, Y. T.; et al. (2003) The structural integrity exerted by N-terminal pyroglutamate is crucial for the cytotoxicity of frog ribonuclease from Rana pipiens. *Nucleic Acids Res. 31*, 5247–5255.
31. Di Fede, G., Catania, M., Morbin, M., Rossi, G., Suardi, S., and Mazzoleni, G.; et al. (2009) A recessive mutation in the APP gene with dominant-negative effect on amyloidogenesis. *Science 323*, 1473–1477.
32. Tartaglia, G. G., Pechmann, S., Dobson, C. M., and Vendruscolo, M. (2007) Life on the edge: a link between gene expression levels and aggregation rates of human proteins. *Trends Biochem. Sci. 32*, 204–206.
33. Cynis, H., Schilling, S., Bodnar, M., Hoffmann, T., Heiser, U., and Saido, T. C.; et al. (2006) Inhibition of glutaminyl cyclase alters pyroglutamate formation in mammalian cells. *Biochim. Biophys. Acta 1764*, 1618–1625.